

KANGURA: Kolmogorov-Arnold Network-Based Geometry-Aware Learning with Unified Representation Attention for 3D Modeling of Complex Structures

Mohammad Reza Shafie^{*1}, Morteza Hajiabadi^{*2}, Hamed Khosravi^{*3}, and Imtiaz Ahmed³

¹Department of Electrical Engineering, Iran University of Science and Technology, Tehran, Iran

²Department of Computer Engineering, Iran University of Science and Technology, Tehran, Iran

³Department of Industrial & Management Systems Engineering, West Virginia University, Morgantown, WV 26505, USA

Abstract

Microbial Fuel Cells (MFCs) offer a promising pathway for sustainable energy generation by converting organic matter into electricity through microbial processes. A key factor influencing MFC performance is the anode structure, where design and material properties play a crucial role. Existing predictive models struggle to capture the complex geometric dependencies necessary to optimize these structures. To solve this problem, we propose KANGURA: Kolmogorov-Arnold Network-Based Geometry-Aware Learning with Unified Representation Attention. KANGURA introduces a new approach to three-dimensional (3D) machine learning modeling. It formulates prediction as a function decomposition problem, where Kolmogorov-Arnold Network (KAN)-based representation learning reconstructs geometric relationships without conventional multi-layer perceptron (MLP). To refine spatial understanding, geometry-disentangled representation learning separates structural variations into interpretable components, while unified attention mechanisms dynamically enhance critical geometric regions. Experimental results demonstrate that KANGURA outperforms over 25 state-of-the-art (SOTA) models on the ModelNet40 benchmark dataset, achieving 94.2% accuracy, and excels in a real-world MFC anode structure problem with 97% accuracy. This establishes KANGURA as a robust framework for 3D geometric modeling, unlocking new possibilities for optimizing complex structures in advanced manufacturing and quality-driven engineering applications.

1 Introduction

Microbial Fuel Cells (MFCs) have gained increasing attention as a promising sustainable energy technology, utilizing microorganisms to convert organic matter into electricity. This dual-purpose system not only generates renewable energy but also aids in wastewater treatment and organic waste management [1]. A key factor influencing MFC efficiency is the anode structure, which plays a crucial role in electron transfer from microorganisms to the circuit. Optimizing anode design

^{*}These authors are joint first authors and contributed equally to this work.

can significantly enhance power generation and improve substrate degradation rates [2]. When effectively implemented at scale, MFC technology offers a broad range of applications, including electricity generation, biohydrogen production, wastewater treatment, biosensing, hazardous waste remediation, and integration into robotic systems[3].

Three-dimensional (3D) models enable detailed simulation of fluid flow and ion transport within complex anode geometries by solving governing equations over volumetric meshes. This allows identification of localized performance issues critical for optimizing MFC anode design. However, their high computational cost limits their practicality for iterative structural prediction.[4]. By incorporating kinetics and electrochemical equations such as Monod and Butler–Volmer formulations, 3D models capture spatial heterogeneities in substrate utilization and electron transfer. Despite the computational demands, they remain essential tools for guiding the rational design of high-performance MFC architectures[5].

Despite its potential, predicting the optimal 3D structure of MFC anodes remains a challenge. The interplay between geometric complexity, material constraints, and microbial interactions makes it difficult to develop models that accurately capture these relationships. Many traditional approaches struggle to balance the intricate trade-offs between anode shape, material composition, and biofilm formation, often resulting in suboptimal designs [6]. Furthermore, the performance of anodes is highly dependent on material properties, as variations can directly impact biofilm growth and electron transfer efficiency [7].

Recent advancements in artificial intelligence (AI) and machine learning (ML) offer new possibilities for improving predictive modeling in this area. AI-based models can analyze large experimental datasets to detect patterns and optimize design parameters, ultimately aiding in the development of more efficient anode structures [8, 9]. For instance, some studies have explored the use of ML and deep learning techniques to predict the performance of different anode materials and configurations, demonstrating how these approaches could reshape the future of MFC design [6, 10]. An artificial neural network integrated with an optimization algorithm has been applied to identify optimal yeast and wastewater concentrations for maximizing power output and COD removal in a microalgae-based MFC. This AI-driven approach has demonstrated superior predictive accuracy compared to conventional analytical methods and has led to improved overall performance. Data-driven optimization of this kind has enabled rapid identification of ideal operating conditions, providing valuable input for guiding more detailed 3D simulations[11].

ML models have revolutionized 3D structure prediction across engineering and materials science, with deep learning architectures playing a key role in these advancements. Graph Neural Networks (GNNs) have proven particularly effective in modeling spatial relationships, as they represent materials and their interactions as graph structures [12]. This capability allows GNNs to process intricate relationships within 3D objects. Additionally, PointNet and its extensions have been instrumental in directly handling point cloud data, enabling efficient classification and segmentation of 3D objects without voxelization [13]. PointNet++ has further enhanced this capability by incorporating hierarchical feature learning, which better captures fine-grained local structures, making it more suitable for complex geometric modeling tasks[14].

However, the existing methods for predicting MFC anode structures face several limitations, primarily related to their inability to effectively capture the complex geometries and interactions inherent in 3D designs [15]. Traditional physics-based models often rely on simplifying assumptions that fail to capture the full complexity of material and geometric interactions, leading to imprecise predictions [16]. While GNNs excel at capturing relationships within large-scale graphs, they can

be computationally demanding, limiting their use in real-time applications [17]. Similarly, while PointNet efficiently processes raw 3D data, its reliance on global pooling may cause a loss of important local geometric details [18].

To address these limitations, attention-based models have emerged as an alternative, dynamically prioritizing key features in the data to improve accuracy and robustness. Specifically, unified attention mechanism, which dynamically focuses on relevant features during training, enables models to filter out noise and prioritize useful information. This selective focus has significantly improved model generalization in complex and noisy environments[19]. Another promising approach in predictive modeling is the Kolmogorov-Arnold Network (KAN) [20], a neural network architecture designed to approximate complex functions by decomposing input data hierarchically. Based on mathematical theory, KANs combine additive and multiplicative feature interactions, making them suitable for capturing complex relationships in high-dimensional data [21]. This capability in conjunction with attention improves the accuracy of AI-driven models in scientific applications, particularly in materials science and engineering, where nonlinear interactions play a critical role [22]. In addition to these concepts, disentangled representation learning has become increasingly important in geometry-aware AI modeling. This approach allows models to separate different factors of variation within data, leading to more meaningful and interpretable feature representations [13]. Together, these techniques provide a more refined and structured approach to learning complex geometric patterns, making them particularly valuable for 3D structure prediction.

In summary, this paper presents **KANGURA**, a novel model for 3D structure prediction and provides the following primary contributions:

- **KAN-based decomposition**, which improves function approximation and enhances the accuracy of complex 3D predictions.
- **Geometry-disentangled representation learning**, allowing the model to better capture structural variations by separating different geometric features.
- **Unified attention mechanisms**, which refine spatial awareness and help the model focus on the most relevant details for more reliable predictions.
- **Evaluation on both synthetic and real-world datasets**, demonstrating its effectiveness on the ModelNet40 benchmark and a real-world MFC anode structure with complex geometry.

Table 1: Comparison of feature capabilities across different model types for 3D modeling

Feature / Model Type	Geometric Awareness	Global Geometric Understanding	Local Geometric Understanding	Spatial Attention	Handles Complex Functions	Function Decomposition
Physics-Based Models [23, 24, 25, 26]	x	x	x	x	x	x
Traditional ML Models [27, 28, 29, 30]	x	x	x	x	x	x
Deep Learning-Based Models [31, 32, 33, 34]	✓	✓	✓	x	✓	x
Graph Neural Networks [35, 36, 37, 38]	✓	✓	✓	x	✓	x
PointNet Variants [39, 40, 41, 42]	✓	✓	✓	x	x	x
KANGURA (Our Model)	✓	✓	✓	✓	✓	✓

Table 1 provides a comparative analysis of different model types based on their ability to capture geometric features and handle complex functions. Unlike traditional ML and physics-based models,

deep learning-based approaches demonstrate improved geometric awareness. However, they lack function decomposition and spatial attention, which are fully addressed by **KANGURA**. Our model uniquely captures and refines the holistic and complementary 3D geometric semantics, making it more effective for complex manufacturing designs.

The rest of the paper is organized as follows. The problem statement and dataset understanding are summarized in Section 2. Section 3 describes the preliminaries, definitions, and high-level steps of our proposed method. Section 4 highlights computational results, and the comparative study. Finally, Section 5 provides concluding remarks and suggestions for future research.

2 Problem Setup

In this section, we define the problem of manufacturability classification in additive manufacturing. Specifically, our aim is to identify whether a given 3D design can be successfully manufactured, considering its geometric and structural attributes.

2.1 Problem Statement

Additive manufacturing (AM) enables the creation of complex designs and functional assemblies, providing new possibilities for product development. A key difficulty, particularly for novice users of 3D fabrication technologies, is to ensure that their designs are compatible with the capabilities of the selected manufacturing process [43]. This challenge arises because of the intricate relationship between the design’s geometry, material properties, and the manufacturing process capabilities. Manufacturability is influenced by various factors, including geometric complexity, structural feasibility, and material limitations. This challenge is particularly critical in applications such as microbial fuel cell (MFC) anodes, where intricate 3D structures are integral to performance. This research is important, not only because the design knowledge of manufacturers can be improved, but also because design exploration can be expanded and expedited. When feasible designs are generated faster, manufacturers can focus on designs with improved manufacturability, higher feasibility, and optimized performance. Addressing this issue through automated classification methods is essential to improving the design-to-production workflow, saving time, reducing costs, and enhancing design capabilities in various industries.

Figure 1 illustrates the problem setup for addressing manufacturability classification in the context of 3D designs. Panel (a) of Figure 1 shows the training phase, where manufacturable designs are represented by feasible geometries that can be physically fabricated. Panel (b) displays non-manufacturable designs, which are characterized by impractical features that hinder production. Finally, panel (c) represents the testing phase, where the trained model is applied to unseen 3D designs to predict their manufacturability. This workflow emphasizes the goal of automating the assessment process to accelerate validation and improve design outcomes.

2.2 Case Study

To address this challenge, a dataset consisting of 1,000 3D models has been curated, including 300 manufacturable designs and 700 non-manufacturable designs. Each design is represented by its geometric and structural attributes, capturing the essential features that influence manufacturability.

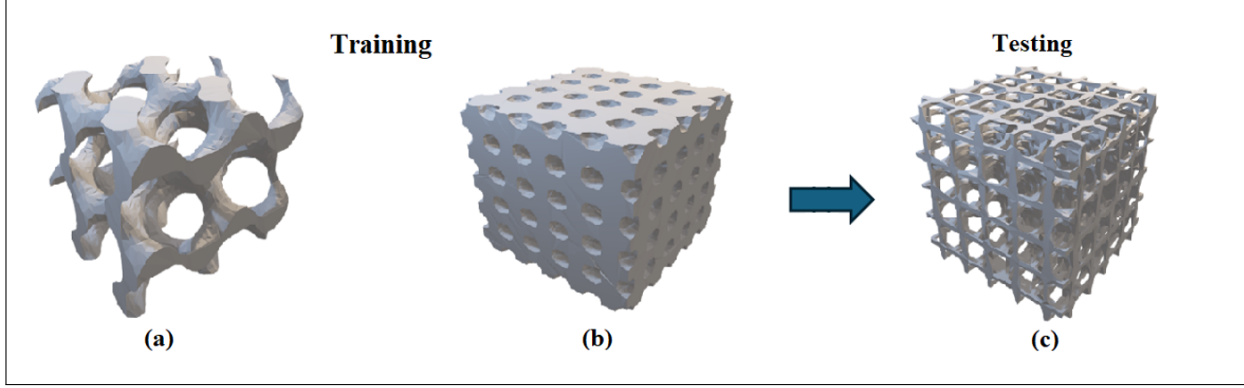


Figure 1: Illustration of the manufacturability classification process for 3D designs. Panel (a) shows manufacturable designs with feasible geometries. Panel (b) displays non-manufacturable designs with impractical features. Panel (c) demonstrates the testing phase, where the trained model is applied to predict the manufacturability of new designs.

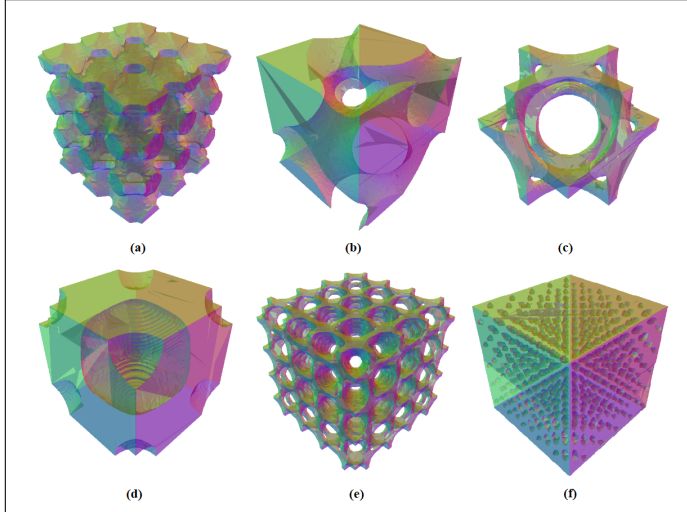


Figure 2: 3D visualizations of additional manufacturable and non-manufacturable designs, highlighting the internal structure of each object. Panels (a), (b), and (c) represent manufacturable designs, where the internal geometries are feasible for production. Panels (d), (e), and (f) display non-manufacturable designs, characterized by impractical internal features that prevent physical fabrication.

This class-imbalanced dataset reflects the reality of design data, where non-manufacturable configurations are more prevalent. The task is to develop a robust classification model capable of learning from these features and accurately distinguishing between manufacturable and non-manufacturable designs. The diversity in geometric complexity and structural variation within the dataset makes it a suitable benchmark for evaluating classification system performance. For instance, as shown in Figure 2, manufacturable designs (panels (a), (b), and (c)) exhibit feasible internal geometries, while non-manufacturable designs (panels (d), (e), and (f)) display impractical internal features that

complicate their fabrication.

To effectively capture the spatial and structural properties of each design, point clouds are used as the primary 3D representation format in this study. Point clouds offer a high-fidelity and compact representation of object geometry, preserving fine-grained spatial details without requiring surface meshing or volumetric modeling. This enables the classification system to learn directly from raw geometric patterns, which are critical in assessing design feasibility. Their viewpoint-agnostic nature also allows consistent feature extraction across different orientations, enhancing the model’s generalization capability. As illustrated in Figure 3, point cloud renderings from multiple angles reveal the internal characteristics that influence manufacturability. Panels (a), (b), and (c) show different perspectives of manufacturable designs, each exhibiting coherent and production-ready internal structures. In contrast, panels (d), (e), and (f) depict non-manufacturable designs with irregular or impractical geometries that violate fabrication constraints.

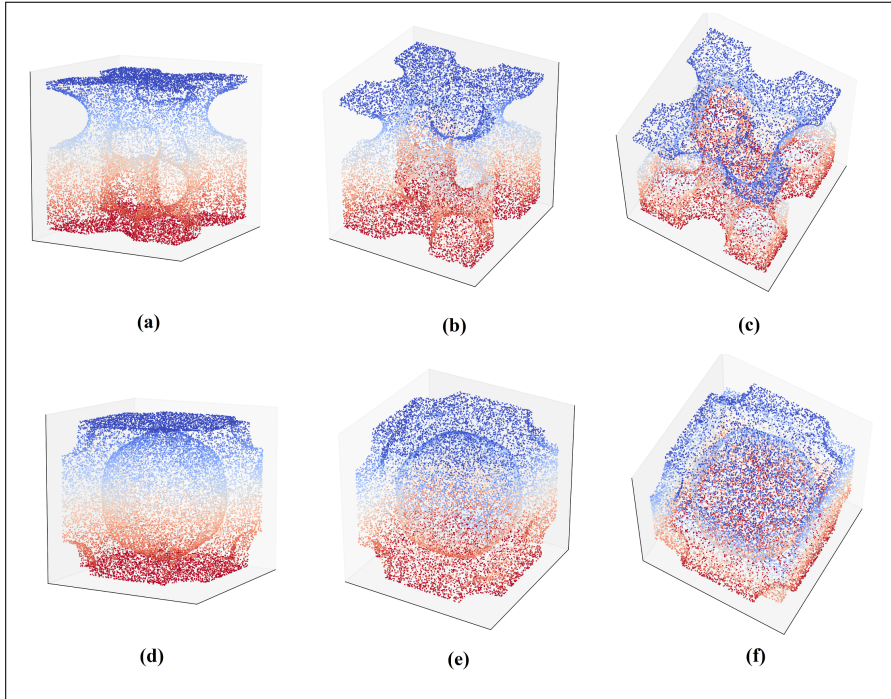


Figure 3: Multi-view point cloud visualizations of 3D designs used for manufacturability classification. Panels (a)–(c) show manufacturable designs with feasible internal geometries. Panels (d)–(f) illustrate non-manufacturable designs featuring impractical structural configurations that hinder fabrication.

3 Methodology

In this section, the high-level process of the proposed method is explained. The methodology shown in Algorithm 1 consists of five key steps: graph construction, geometry disentanglement, function approximation via KAN, attention-based feature refinement, and final feature fusion.

This framework is designed to learn a robust and enhanced geometric representation from 3D point cloud data, which can then be used for classification tasks such as determining manufacturability. The overall process, detailed below, transforms raw coordinates into a rich feature set that captures complex structural relationships.

Algorithm 1 Overall Steps of KANGURA: Kolmogorov-Arnold Network-Based Geometry-Aware Learning with Unified Representation Attention

- 1: **Input:** Point cloud $X \in \mathbb{R}^{N \times C}$ with N points and C features
- 2: **Output:** Enhanced feature representation $Z \in \mathbb{R}^{N \times C'}$

Graph Construction and Spectral Representation

- 3: Compute adjacency matrix $A_{ij} = \exp(-\|x_i - x_j\|^2/\sigma^2)$ if $\|x_i - x_j\| \leq \tau$, else 0. Compute graph Laplacian $L = D - A$ and its decomposition $L = U\Lambda U^T$.

Geometry Disentanglement

- 4: Extract high-frequency sharp variation $X_s = U_{[\lambda_T, \dots, \lambda_N]}^T X$ and low-frequency gentle variation $X_g = U_{[0, \dots, \lambda_T]}^T X$. Apply spectral filtering: $\hat{X}_s = (I - \tilde{A})X_s$, $\hat{X}_g = \tilde{A}X_g$.

KAN Functional Decomposition

- 5: Transform features using hierarchical KAN layers with functional mapping $f(X) = \sum_{q=1}^{2n+1} \Phi_q \left(\sum_{p=1}^n \varphi_{qp}(X_p) \right)$. Compute layer-wise activations $x_{l+1,j} = \sum_{i=1}^{n_l} \varphi_{l,j,i}(x_{l,i})$. The final KAN representation is $KAN(X) = (\Phi_{L-1} \circ \dots \circ \Phi_0)(X)$, applied separately to both sharp and gentle variations: $KAN_s = KAN(\hat{X}_s)$, $KAN_g = KAN(\hat{X}_g)$.

Unified Representation Attention

- 6: Compute attention weights $W_s = \Theta_o(X) \cdot \Theta_s(KAN_s)^T$, $W_g = \Phi_o(X) \cdot \Phi_g(KAN_g)^T$, then refine feature representations as $Y_s = X + W_s(KAN_s)$, $Y_g = X + W_g(KAN_g)$.

Feature Fusion and Output

- 7: Compute final representation $Z = Y_s \oplus Y_g$ and return Z .
-

Graph Construction and Spectral Representation To encode the geometric structure of a 3D point cloud $X \in \mathbb{R}^{N \times C}$, we construct an adjacency matrix $A \in \mathbb{R}^{N \times N}$ based on feature-space proximity:

$$A_{ij} = \begin{cases} \exp\left(-\frac{\|x_i - x_j\|^2}{\sigma^2}\right), & \text{if } \|x_i - x_j\| \leq \tau \\ 0, & \text{otherwise} \end{cases} \quad (1)$$

where σ is the scaling parameter and τ is the distance threshold. This initial step transforms the raw point cloud into a structured graph, enabling the model to process intricate spatial relationships between points rather than treating them as an unordered set.

The graph Laplacian is computed as:

$$L = D - A, \quad L = U\Lambda U^T \quad (2)$$

where D is the degree matrix and U contains the eigenvectors. The computation of the graph Laplacian is critical as its spectral properties (eigenvectors and eigenvalues) form the basis for frequency-based filtering and analysis of the underlying geometry in subsequent steps.

Geometry Disentanglement To separate fine-grained and coarse geometric variations, we partition the spectral domain into sharp and gentle components. High-frequency components (sharp variations) are extracted as:

$$X_s = U_{[\lambda_T, \dots, \lambda_N]}^T X, \quad (3)$$

while low-frequency components (smooth variations) are given by:

$$X_g = U_{[0, \dots, \lambda_T]}^T X. \quad (4)$$

These components are further refined via:

$$\hat{X}_s = (I - \tilde{A})X_s, \quad \hat{X}_g = \tilde{A}X_g, \quad (5)$$

ensuring structured feature disentanglement.

This key step leverages the spectral representation to partition the geometry into more meaningful and interpretable components. The high-frequency "sharp" variations correspond to fine-grained local details like edges and corners, while the low-frequency "gentle" variations represent the coarse, overall shape of the object. By separating these factors of variation, the model can learn from both types of geometric information independently, ensuring that subtle but important details are not overshadowed by the global structure.

KAN for Functional Decomposition Instead of traditional MLPs, KANGURA employs KAN for function approximation. The Kolmogorov-Arnold representation theorem states that any multivariate function $f : \mathbb{R}^n \rightarrow \mathbb{R}$ can be represented as:

$$f(X) = \sum_{q=1}^{2n+1} \Phi_q \left(\sum_{p=1}^n \varphi_{qp}(X_p) \right), \quad (6)$$

where φ_{qp} and Φ_q are learnable univariate functions. The KAN is applied hierarchically as $x_{l+1,j} = \sum_{i=1}^{n_l} \varphi_{l,j,i}(x_{l,i})$, allowing adaptive functional decomposition. According to mathematical theory, KANs can capture complex, non-linear relationships in high-dimensional data more effectively than conventional models. This is particularly valuable for modeling 3D structures where the interplay between geometric features is inherently non-linear. The overall KAN representation is:

$$\text{KAN}(X) = (\Phi_{L-1} \circ \Phi_{L-2} \circ \dots \circ \Phi_0)(X), \quad (7)$$

which enhances feature extraction from the disentangled sharp and gentle variations:

$$KAN_s = \text{KAN}(\hat{X}_s), \quad KAN_g = \text{KAN}(\hat{X}_g). \quad (8)$$

Unified Representation Attention (URA) for Feature Refinement To refine features, KANGURA employs Unified Representation Attention by computing attention weights via bilinear transformations:

$$W_s = \Theta_o(X) \cdot \Theta_s(KAN_s)^T, \quad W_g = \Phi_o(X) \cdot \Phi_g(KAN_g)^T. \quad (9)$$

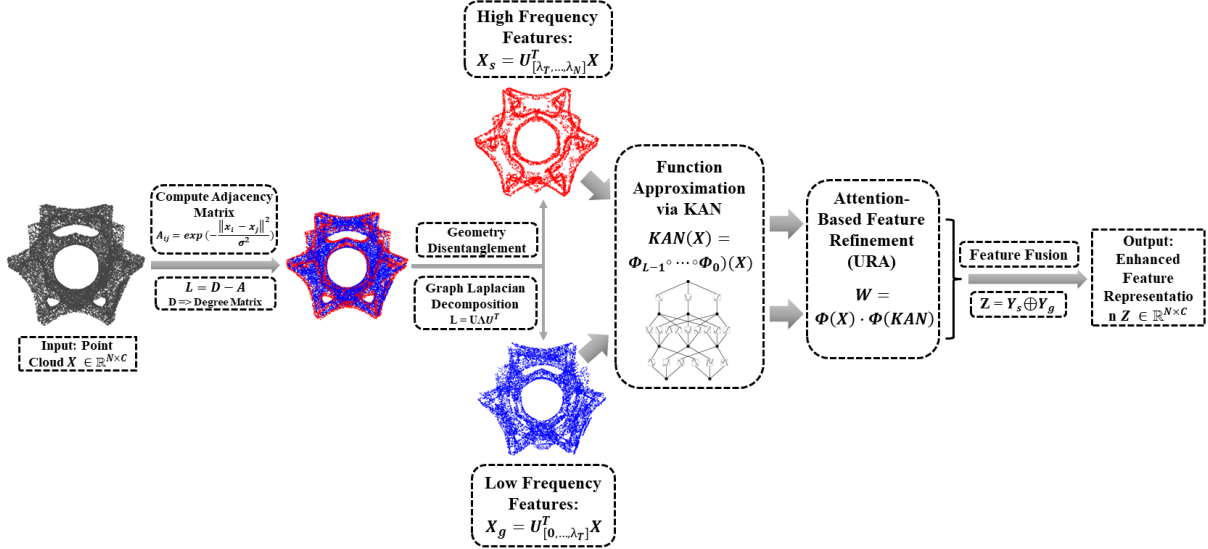


Figure 4: Flowchart of the KANGURA

The feature refinement follows $Y_s = X + W_s KAN_s$, and $Y_g = X + W_g KAN_g$. URA dynamically balances local and global feature aggregation, enhancing feature expressiveness.

Feature Fusion and Final Output The final representation integrates sharp and smooth variations:

$$Z = Y_s \oplus Y_g. \quad (10)$$

This fusion step ensures both fine-grained local detail and global structural coherence are preserved.

This combined representation is then returned as the final output of the model. By ensuring that the holistic and complementary 3D geometric semantics are captured, this final vector is made highly effective for complex classification tasks, such as those in advanced manufacturing. As illustrated in Figure 4, the KANGURA framework handles point cloud data across five essential phases: Graph Construction, Geometry Disentanglement, Function Approximation via KAN, Attention-Based Feature Refinement, and Feature Fusion. The procedure commences with the creation of a graph from the point cloud, utilizing an adjacency matrix and graph Laplacian. Following this, geometry disentanglement is performed, which isolates the high and low-frequency elements of the point cloud's geometry to seize fine-grained geometric details.

In the subsequent stages, KANGURA utilizes Function Approximation via KAN to project the point cloud features into a target output space. These features are then enhanced through an attention-based mechanism that amplifies the significant features. Ultimately, the high and low-frequency features are combined to produce a refined feature representation for use in subsequent tasks. This methodical design allows KANGURA to adeptly model the intricate geometric interdependencies within point cloud data, resulting in better outcomes for applications such as segmentation and classification.

4 Results

This section presents the evaluation of KANGURA on both benchmark and real-world datasets. The first subsection compares its performance against state-of-the-art (SOTA) models on a standard 3D classification benchmark, while the second assesses its effectiveness in the real-world MFC anode structure classification.

Table 2: Comparison of different models on ModelNet40 benchmark dataset

Method	Input Type	Accuracy (%)	Δ from Kangura
SPH	Mesh	68.2	24.5
LFD	View	75.5	17.2
FPNN	Volume	88.4	4.3
PointNet	1K points	89.2	3.5
SCN	1K points	90.0	2.7
MVCNN	View	90.1	2.6
Pairwise	View	90.7	2.0
PointNet++	1K points	90.7	2.0
KCNet	1K points	91.0	1.7
KCNet	Point	91.0	1.7
Kd-Net	Point	91.8	0.9
MeshNet	Mesh	91.9	0.8
PointNet++	5K points + normal	91.9	0.8
3D-GCN	1K points	92.1	0.6
PointCNN	1K points	92.2	0.5
PointWeb	1K points	92.3	0.4
PointConv	1K points + normal	92.5	0.2
FPCConv	1K points	92.5	0.2
Point2Sequence	1K points	92.6	0.1
KANGURA (Ours)	Point	92.7	0.0

4.1 Benchmark Performance

To assess the effectiveness of **KANGURA**, we compare its classification accuracy against over 15 state-of-the-art models on the ModelNet40 benchmark [44], a widely adopted dataset for 3D object recognition comprising 40 shape categories. As presented in Table 2, **KANGURA achieves an accuracy of 92.7%**, outperforming all previously reported methods.

Mesh-based approaches such as SPH (68.2%) and MeshNet (91.9%) illustrate the potential of utilizing explicit surface representations; however, their performance remains below that of leading point-based models, suggesting limitations in capturing fine-grained local structures. View-based methods, including MVCNN (90.1%) and Pairwise (90.7%), aggregate visual information across multiple projections but are inherently constrained by discretized viewpoints and lack of spatial continuity. Volumetric techniques such as FPNN (88.4%) are further hindered by resolution loss and computational overhead associated with voxelization.

In contrast, point-based models consistently yield higher performance, with top contenders including Point2Sequence (92.6%), FPCConv (92.5%), and PointConv (92.5%). **KANGURA** surpasses each of these baselines, with relative improvements of 0.1%, 0.2%, and 0.2%, respectively. These gains underscore the effectiveness of KANGURA’s architectural innovations, the KAN-based functional decomposition and the unified attention mechanism, which jointly contribute to superior

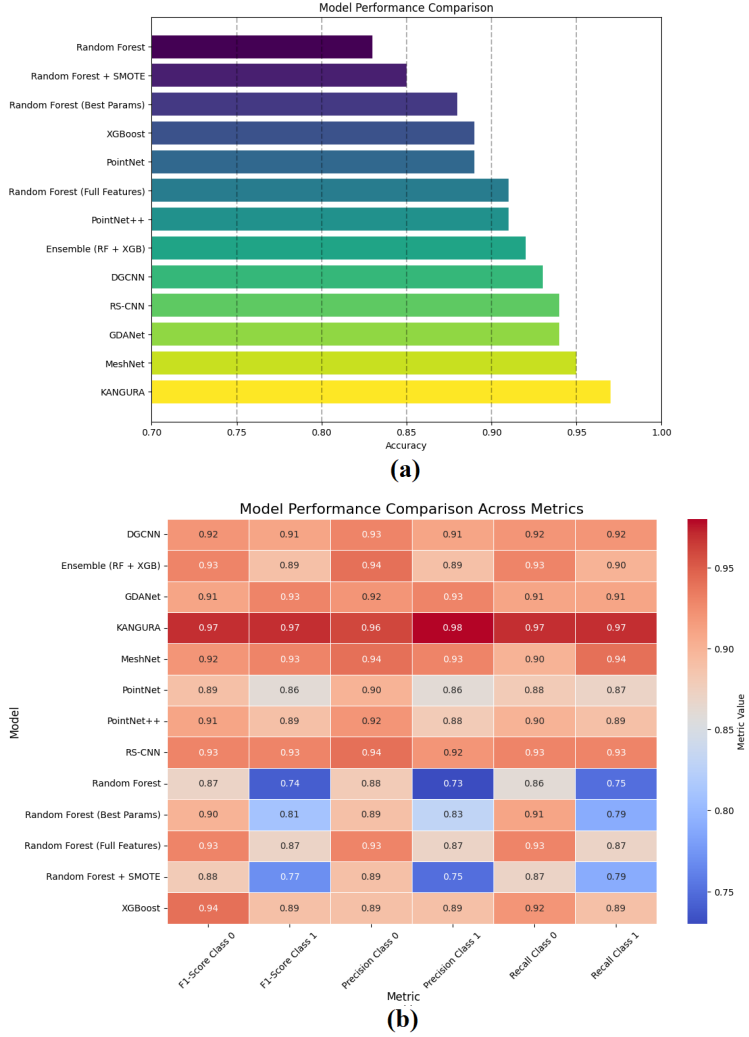


Figure 5: Performance analysis on the real-world data: (a) Accuracy comparison, (b) Heatmap of models performance across Precision, Recall, and F1-Score

geometric feature learning. The resulting enhancement in classification accuracy highlights the model’s robustness and generalizability across diverse input modalities.

The accuracy gains are particularly significant given that earlier models predominantly rely on point-based convolutional networks or graph-based architectures. By introducing a structured function decomposition, **KANGURA outperforms SOTA models** by refining feature extraction and improving spatial awareness. This enables a more robust and precise understanding of 3D structures, ultimately setting a new benchmark in 3D shape recognition. The delta accuracy column strengthens this claim, as it highlights **KANGURA**’s superior ability to generalize and handle variations in input data compared to previous methods.

4.2 Real-world Data

To evaluate KANGURA’s real-world applicability, we tested its performance on the MFC anode structure classification, comparing it with 15 different models including traditional machine learning models using numerical features (e.g., topological and surface ratio features) and deep learning models utilizing 3D mesh data.

Figure 5(a) shows that **KANGURA achieves the highest accuracy (97%)**, surpassing MeshNet (95%) and GDANet (94%), as well as vanilla machine learning models. While ML models capture key geometric properties, they lack the ability to represent local-global spatial dependencies within 3D structures. MeshNet, trained on mesh-based representations, outperforms numerical feature-based approaches but remains constrained by standard convolutions, which limits its ability to fully capture hierarchical geometric relationships. Furthermore, as shown in Figure 5(b), KANGURA maintains superior precision, recall and F1 score in both feasible (Class 1) and infeasible (Class 0) designs, ensuring a robust classification essential to optimize the 3D structure in MFC applications.

5 Conclusion

In this study, we have introduced KANGURA, a novel model addressing the challenges of 3D machine learning in complex advanced manufacturing, where existing models struggle to effectively capture intricate geometric and functional relationships. While MFC anode structure classification serves as an example, KANGURA’s architecture is broadly applicable to quality control and reliability engineering, material design, and structural optimization. Through extensive evaluation, we compared KANGURA against 27 SOTA models on a benchmark dataset and 15 models on real-world data, achieving the highest accuracy across both settings. KANGURA surpasses leading deep learning models, as well as traditional machine learning approaches using geometric and topological features.

By utilizing KAN-based function decomposition, geometry-disentangled representation learning, and unified attention mechanisms, KANGURA achieves superior accuracy, robust classification, and balanced generalization across local and global structural dependencies. These results highlight its potential for data-driven optimization in advanced manufacturing applications, where precise 3D modeling is critical for process efficiency and quality assurance. Future work will explore broader industrial applications, further enhancing its interpretability and scalability across various material science and engineering domains.

References

- [1] Qianyong Zhang, Zhirao Yin, Rui Sun, Chun Zhao, Yongqi Jing, and Fuke Yang. Preparation of new mfc anode and degradation performance of ship’s oily waste waterv. *Academic Journal of Science and Technology*, 11(1):31–35, 2024.
- [2] Dang-Trang Nguyen and Kozo Taguchi. Comparative study of zncl2-activated and steam-activated carbons used in the anode of microbial fuel cells. *IEEJ Transactions on Electrical and Electronic Engineering*, 15(2):313–314, 2020.

- [3] R. Chakma, M. K. Hossain, P. Paramasivam, R. Bousbih, M. Amami, G. I. Toki, and others. Recent applications, challenges, and future prospects of microbial fuel cells: a review. *Global Challenges*, 9(5):2500004, 2025.
- [4] Taylor Kesler. *Comparing 1D, 2D, and 3D Hydraulic Models in Urban Flooding Applications*. Master's thesis, Utah State University, 2023. All Graduate Theses and Dissertations, Spring 1920 to Summer 2023, 8691.
- [5] Dipak A. Jadhav, Alessandro A. Carmona-Martínez, Ashvini D. Chendake, Soumya Pandit, and Deepak Pant. Modeling and optimization strategies towards performance enhancement of microbial fuel cells. *Bioresource Technology*, 320:124256, 2021.
- [6] Mojeed Opeyemi Oyedeleji, Abdullah Alharbi, Mujahed Aldhaifallah, and Hegazy Rezk. Optimal data-driven modelling of a microbial fuel cell. *Energies*, 16(12):4740, 2023.
- [7] B Li, Z Zhao, Z Weng, Y Fang, W Lei, D Zhu, H Jiang, MN Bin Mohtar, and I bin Abdul Halin. Modification of ppy-nw anode by carbon dots for high-performance mini-microbial fuel cells. *Fuel Cells*, 20(2):203–211, 2020.
- [8] Hamed Farahani, Mostafa Ghasemi, Mehdi Sedighi, and Nitin Raut. Employing artificial intelligence for enhanced microbial fuel cell performance through wolf vitamin solution optimization. *Sustainability*, 16(15):6468, 2024.
- [9] Luis Erick Coy-Aceves and Benito Corona-Vasquez. Bibliometric analysis of artificial intelligence algorithms used for microbial fuel cell research. *Water Practice & Technology*, 17(10):2071–2082, 2022.
- [10] Tanay Panja and Priyanka Meharia. Enhancing microbial fuel cell performance prediction and iot integration using machine learning and renewable energy. *Journal of Strategic Innovation and Sustainability*, 19(1):81–90, 2024.
- [11] Enas Taha Sayed, Hegazy Rezk, Mohammad Ali Abdelkareem, and A.G. Olabi. Artificial neural network based modelling and optimization of microalgae microbial fuel cell. *International Journal of Hydrogen Energy*, 52:1015–1025, 2024.
- [12] Iyyakutti Iyappan Ganapathi, Sajid Javed, Robert Bob Fisher, and Naoufel Werghi. Graph based texture pattern classification. In *2022 8th International Conference on Virtual Reality (ICVR)*, pages 363–369. IEEE, 2022.
- [13] Yue Wang, Yongbin Sun, Ziwei Liu, Sanjay E Sarma, Michael M Bronstein, and Justin M Solomon. Dynamic graph cnn for learning on point clouds. *ACM Transactions on Graphics (tog)*, 38(5):1–12, 2019.
- [14] Qi Charles Ruizhongtai, Yi Li, Su Hao, and Guibas Leonidas J PointNet+. Deep hierarchical feature learning on point sets in a metric space. *Advances in Neural Information Processing Systems*, 30, 2023.
- [15] Abhishek Kar, Shubham Tulsiani, Joao Carreira, and Jitendra Malik. Category-specific object reconstruction from a single image. In *Proceedings of the IEEE conference on computer vision and pattern recognition*, pages 1966–1974, 2015.

- [16] Rishi Rajalingham, Elias B Issa, Pouya Bashivan, Kohitij Kar, Kailyn Schmidt, and James J DiCarlo. Large-scale, high-resolution comparison of the core visual object recognition behavior of humans, monkeys, and state-of-the-art deep artificial neural networks. *Journal of Neuroscience*, 38(33):7255–7269, 2018.
- [17] Xinyi Liu, Baofeng Zhang, and Na Liu. The graph neural network detector based on neighbor feature alignment mechanism in lidar point clouds. *Machines*, 11(1):116, 2023.
- [18] Jonathan Schmidt, Love Pettersson, Claudio Verdozzi, Silvana Botti, and Miguel AL Marques. Crystal graph attention networks for the prediction of stable materials. *Science advances*, 7(49):eabi7948, 2021.
- [19] Hongdou Yao, Xuejie Zhang, Xiaobing Zhou, and Shengyan Liu. Parallel structure deep neural network using cnn and rnn with an attention mechanism for breast cancer histology image classification. *cancers*, 11(12):1901, 2019.
- [20] Ziming Liu, Yixuan Wang, Sachin Vaidya, Fabian Ruehle, James Halverson, Marin Soljačić, Thomas Y Hou, and Max Tegmark. Kan: Kolmogorov-arnold networks. *arXiv preprint arXiv:2404.19756*, 2024.
- [21] Lisheng He and Sudeep Bhatia. Complex economic decisions from simple neurocognitive processes: The role of interactive attention. *Proceedings of the Royal Society B*, 290(1992):20221593, 2023.
- [22] Anthony I Jang, Ravi Sharma, and Jan Drugowitsch. Optimal policy for attention-modulated decisions explains human fixation behavior. *Elife*, 10:e63436, 2021.
- [23] Philipp Moser, Wolfgang Fenz, Stefan Thumfart, Isabell Ganitzer, and Michael Giretzlehner. Modeling of 3d blood flows with physics-informed neural networks: comparison of network architectures. *Fluids*, 8(2):46, 2023.
- [24] Arvind T Mohan, Dima Tretiak, Misha Chertkov, and Daniel Livescu. Spatio-temporal deep learning models of 3d turbulence with physics informed diagnostics. *Journal of Turbulence*, 21(9-10):484–524, 2020.
- [25] Jiaheng Kang, Gaoyang Li, Yue Che, Xiran Cao, Mingyu Wan, Jing Zhu, Mingyao Luo, and Xuelan Zhang. Four-dimensional hemodynamic prediction of abdominal aortic aneurysms following endovascular aneurysm repair combining physics-informed pointnet and quadratic residual networks. *Physics of Fluids*, 36(8), 2024.
- [26] Haiming Zhang, Xinlin Xia, Ze Wu, and Xiaolei Li. Physics-informed graph neural network based on the finite volume method for steady incompressible laminar convective heat transfer. *Physics of Fluids*, 37(1), 2025.
- [27] Yixing Huang, Yanye Lu, Oliver Taubmann, Guenter Lauritsch, and Andreas Maier. Traditional machine learning for limited angle tomography. *International journal of computer assisted radiology and surgery*, 14:11–19, 2019.
- [28] Sahar K Hussin, Yasser M Omar, Salah M Abdelmageid, and Mahmoud I Marie. Traditional machine learning and big data analytics in virtual screening: a comparative study. *International Journal of Advanced Computer Research*, 10(47):72–88, 2020.
- [29] Izabela Rojek, Dariusz Mikołajewski, Piotr Kotlarz, Krzysztof Tyburek, Jakub Kopowski, and Ewa Dostatni. Traditional artificial neural networks versus deep learning in optimization of material aspects of 3d printing. *Materials*, 14(24):7625, 2021.

- [30] Dong Nguyen, Hoang Nguyen, Hong Ong, Hoang Le, Huong Ha, Nguyen Thanh Duc, and Hoan Thanh Ngo. Ensemble learning using traditional machine learning and deep neural network for diagnosis of alzheimer’s disease. *IBRO Neuroscience Reports*, 13:255–263, 2022.
- [31] Yin Zhou and Oncel Tuzel. Voxelnets: End-to-end learning for point cloud based 3d object detection. In *Proceedings of the IEEE conference on computer vision and pattern recognition*, pages 4490–4499, 2018.
- [32] Saifullahi Aminu Bello, Shangshu Yu, Cheng Wang, Jibril Muhammad Adam, and Jonathan Li. Deep learning on 3d point clouds. *Remote Sensing*, 12(11):1729, 2020.
- [33] Mutian Xu, Junhao Zhang, Zhipeng Zhou, Mingye Xu, Xiaojuan Qi, and Yu Qiao. Learning geometry-disentangled representation for complementary understanding of 3d object point cloud. In *Proceedings of the AAAI conference on artificial intelligence*, volume 35, pages 3056–3064, 2021.
- [34] Yutong Feng, Yifan Feng, Haoxuan You, Xibin Zhao, and Yue Gao. Meshnet: Mesh neural network for 3d shape representation. In *Proceedings of the AAAI conference on artificial intelligence*, volume 33, pages 8279–8286, 2019.
- [35] Xinshuo Weng, Yongxin Wang, Yunze Man, and Kris M Kitani. Gnn3dmot: Graph neural network for 3d multi-object tracking with 2d-3d multi-feature learning. In *Proceedings of the IEEE/CVF Conference on Computer Vision and Pattern Recognition*, pages 6499–6508, 2020.
- [36] Zhiming Zou and Wei Tang. Modulated graph convolutional network for 3d human pose estimation. In *Proceedings of the IEEE/CVF international conference on computer vision*, pages 11477–11487, 2021.
- [37] An Ping Song, Xin Yi Di, Xiao Kang Xu, and Zi Heng Song. Meshgraphnet: An effective 3d polygon mesh recognition with topology reconstruction. *IEEE Access*, 8:205181–205189, 2020.
- [38] Xin Wei, Ruixuan Yu, and Jian Sun. View-gcn: View-based graph convolutional network for 3d shape analysis. In *Proceedings of the IEEE/CVF Conference on Computer Vision and Pattern Recognition*, pages 1850–1859, 2020.
- [39] Yibo Cao, Shun Liu, Pengfei Zhao, and Haiwen Zhu. Rp-net: A pointnet++ 3d face recognition algorithm integrating rops local descriptor. *IEEE Access*, 10:91245–91252, 2022.
- [40] Lin Zhao and Wenbing Tao. Jsnet++: Dynamic filters and pointwise correlation for 3d point cloud instance and semantic segmentation. *IEEE Transactions on Circuits and Systems for Video Technology*, 33(4):1854–1867, 2022.
- [41] Shivanand Venkanna Sheshappanavar and Chandra Kambhamettu. A novel local geometry capture in pointnet++ for 3d classification. In *Proceedings of the IEEE/CVF Conference on Computer Vision and Pattern Recognition Workshops*, pages 262–263, 2020.
- [42] Yi Tian, Kai Wang, Gengchen Lv, Yaohong Qu, Chengxiang Wang, and Kaijiang Wang. Research on semantic segmentation method of 3d point cloud for uav landing. In *International Conference on Advanced Image Processing Technology (AIPT 2024)*, volume 13257, pages 193–199. SPIE, 2024.
- [43] Ying Zhang and Yaoyao Fiona Zhao. A web-based automated manufacturability analyzer and recommender for additive manufacturing (mar-am) via a hybrid machine learning model. *Expert Systems with Applications*, 199:117189, 2022.

- [44] Zhirong Wu, Shuran Song, Aditya Khosla, Fisher Yu, Linguang Zhang, Xiaoou Tang, and Jianxiong Xiao. 3d shapenets: A deep representation for volumetric shapes. In *Proceedings of the IEEE conference on computer vision and pattern recognition*, pages 1912–1920, 2015.